# Dijet cross sections in ep collisions: who is afraid of symmetric cuts?

Jiří Chýla, Kamil Sedlák

Institute of Physics, Academy of Sciences of the Czech Republic, 18221 Na Slovance 2, Prague 8, Czech Republic

### Abstract

Three widely used scenaria for defining cuts on transverse energies of jets in ep collisions are discussed. All of them are shown to suffer from the same sort of unphysical behaviour when the cut regions are subject to additional constraints. This feature is inherent in the very way dijet cross sections are defined and cannot be avoided. In particular, the symmetric cut scenario is shown to be equally suitable for the comparison with NLO QCD calculations as the asymmetric or sum-like ones.

Key words: QCD, perturbation theory, jet cross sections, infrared safety *PACS*: 12.38.Bx, 12.38.Qk, 13.60.Hb

In analyzing the data on inclusive jet production in electron-proton collisions some lower cut  $E_c$  (at HERA typically  $E_c \gtrsim 5$  GeV) on the transverse energy of jets is necessary for experimental as well as theoretical reasons. In parts of the multijet phase space the cut on the transverse energies of two jets with highest  $E_T$  may, however, get into conflict with the infrared safety of the corresponding cross sections.

In the next-to-leading QCD calculations of single and dijet cross sections there are at most three final state partons, which combine to two or three jets. Ordering the jets according to their transverse energies in  $\gamma^*p$  center-of-mass system  $(E_T^{(1)} \geq E_T^{(2)} \geq E_T^{(3)})$ , the corresponding phase space, marked by the upper and lower solid straight lines in Figs. 2-4, is given by the inequality  $E_T^{(1)}/2 \leq E_T^{(2)} \leq E_T^{(1)}$ . This constraint, given by pure kinematics, must then be combined with additional conditions that might be imposed on jets for experimental and theoretical reasons. Phrasing the constraint on allowed part of phase space in terms of  $E_T^{(1)}, E_T^{(2)}$  does not, however, imply that only genuine dijet variables must be investigated or only the first two jets taken into account. For instance, the inclusive single jet cross section gets in principle contribution even from the third jet.

The aim of this letter is to argue that there is no way of choosing the cuts on  $E_T^{(1)}$ ,  $E_T^{(2)}$  that would be free from the sort of unphysical behaviour of cross sections noted in [1]. We shall illustrate our claims on the calculation of cross sections in ep collisions at HERA in the region relevant for the analysis in [2]

$$2 \le Q^2 \le 80 \text{ GeV}, \quad 0.1 \le y \le 0.85, \quad E_c = 5 \text{ GeV},$$
 (1)

but they are clearly of more general validity. All calculations reported below were obtained by means DISENT NLO Monte-Carlo program [3] using CTEQ6M set of parton distribution functions (PDF) of the proton. For dijet events there are three classes of distributions that can be measured:

• separate distributions of transverse energies and pseudorapidities

$$\frac{\mathrm{d}\sigma}{\mathrm{d}E_T^{(1)}}, \quad \frac{\mathrm{d}\sigma}{\mathrm{d}E_T^{(2)}}, \quad \frac{\mathrm{d}\sigma}{\mathrm{d}\eta^{(1)}}, \quad \frac{\mathrm{d}\sigma}{\mathrm{d}\eta^{(2)}}, \tag{2}$$

• their sums, corresponding to distributions of what is called in [4] "trigger jets",

$$\frac{\mathrm{d}\sigma}{\mathrm{d}E_T} \equiv \frac{\mathrm{d}\sigma}{\mathrm{d}E_T^{(1)}} + \frac{\mathrm{d}\sigma}{\mathrm{d}E_T^{(2)}}, \quad \frac{\mathrm{d}\sigma}{\mathrm{d}\eta} \equiv \frac{\mathrm{d}\sigma}{\mathrm{d}\eta^{(1)}} + \frac{\mathrm{d}\sigma}{\mathrm{d}\eta^{(2)}}, \tag{3}$$

• or the distributions of some of the combinations characterizing the whole event, like their mean values  $\overline{E}_T \equiv (E_T^{(1)} + E_T^{(2)})/2$  and  $\overline{\eta} \equiv (\eta^{(1)} + \eta^{(2)})/2$ 

$$\frac{\mathrm{d}\sigma}{\mathrm{d}\overline{E}_T}, \quad \frac{\mathrm{d}\sigma}{\mathrm{d}\overline{\eta}},$$
 (4)

but one is free to use general combinations as well.

Symmetric cut scenario

In this scenario the same cut is imposed on both jets

$$E_T^{(1)} \ge E_c, \quad E_T^{(2)} \ge E_c.$$
 (5)

This is quite appropriate for the comparison of data with lowest QCD calculations because the latter involve binary partonic hard processes which lead (in diparton rest frame) to two partons with the same transverse energies. Its use in NLO QCD calculations of dijet cross sections has been questioned in [1] observing that it leads to unphysical behaviour of the cross section  $\sigma_{sym}(\Delta)$  corresponding to the integral over the region defined in (5) supplemented with an additional constraint  $E_T^{(1)} \geq E_c + \Delta$ , represented graphically by the red dotted curve in the upper right plot of Fig. 1. The resulting dependence, displayed as red solid curve in the left part of Fig. 1, implies that for  $\Delta$  approaching zero,  $\sigma_{sym}(\Delta)$  decreases despite the fact that the corresponding phase space increases. The source of this unphysical behaviour can be traced back to the fact that at the order  $\alpha \alpha_s^2$  perturbative QCD does not yield a well-defined result for the double differential cross section  $d\sigma/dE_T^{(1)}dE_T^{(2)}$  when  $E_T^{(1)} = E_T^{(2)}$ .

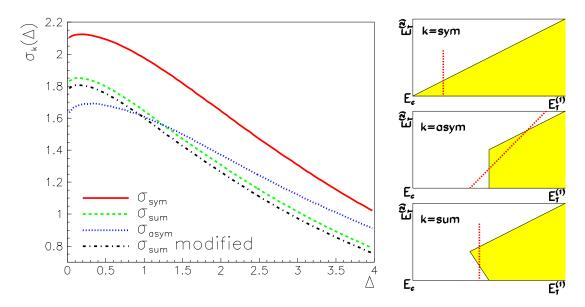


Fig. 1. The dependence of  $\sigma_k(\Delta)$  on the parameter  $\Delta$  restricting the regions defined in (5,6,8) and marked in yellow, to the right of the red dotted curves.

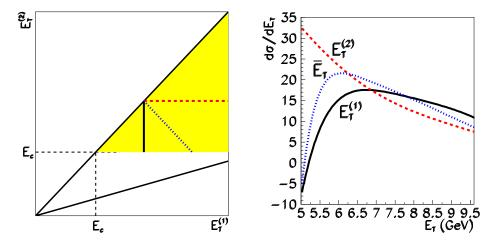


Fig. 2. Left: symmetric cuts scenario,  $E_c=5$  GeV. The solid, dotted and dashed lines correspond to fixed values of  $E_T^{(1)}$ ,  $\overline{E}_T$  and  $E_T^{(2)}$ . As they approach  $E_c$  from above the lengths of the former two decrease, whereas that of  $E_T^{(2)}$  increases. Right: corresponding distributions of  $E_T^{(1)}$  (solid),  $E_T^{(2)}$  (dashed) and  $\overline{E}_T$  (dotted).

This comes from the fact that at this order there are mass divergencies of the virtual corrections that must be cancelled by those of the real emissions. For a quantity to be calculable in perturbative QCD one must thus allow for integration over sufficient part of the three parton phase space, where  $E_T^{(2)} < E_T^{(1)}$ .

To understand better the origin of the behaviour of  $\sigma_{sym}(\Delta)$  we plot in Fig. 2 the distributions of  $E_T^{(1)}$ ,  $E_T^{(2)}$  and  $\overline{E}_T$  for  $E_c = 5$  GeV. As expected, the distributions of both  $E_T^{(1)}$  and  $\overline{E}_T$  turn negative for  $E_T^{(1)}$  or  $\overline{E}_T$  close to  $E_c = 5$  GeV because of the small volume (represented in left parts of Figs. 2-4 by the length of perpendicular solid or oblique dotted lines) of phase space available for the real parton emission. In fact both these distributions diverge

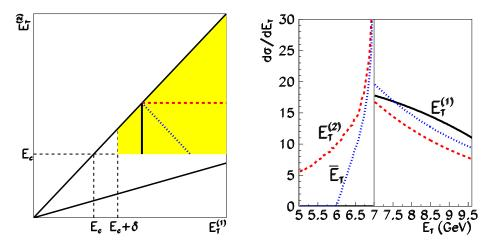


Fig. 3. The same as in Fig. 2 but for asymmetric cuts scenario with  $E_c = 5$  GeV and  $\delta = 2$  GeV.

to  $-\infty$  as  $E_T^{(1)}$  or  $\overline{E}_T$  approach  $E_c$  from above, thereby causing  $\sigma_{sym}(\Delta)$  and  $\sigma_{sum}(\Delta)$  in Fig. 1 to bend down for small  $\Delta$ . On the other hand  $d\sigma/dE_T^{(2)}$  grows monotonously with decreasing  $\Delta$ , reflecting the fact that even for  $E_T^{(2)} = E_c$  there is plenty of phase space (represented in the left parts of Figs. 2-4 by the dash horizontal lines) available for the real gluon emission because  $E_T^{(1)}$  can be anywhere above it. Note that the integrals over all three distributions in Fig. 2 are finite and equal as they correspond to three different ways of performing the integral over the same region defined in (5). There is thus no reason to reject the symmetric cut scenario for the comparison of data with NLO QCD, but for  $E_T$  close to  $E_c$ , one should compare the distributions of  $E_T^{(2)}$ , rather than those of  $E_T^{(1)}$ .

#### Asymmetric cut scenario

To avoid the above unphysical behaviour of  $\sigma_{sym}$  the asymmetric cut scenario

$$E_T^{(1)} > E_c + \delta, \quad E_T^{(2)} > E_c,$$
 (6)

where  $\delta \geq 0$ , was suggested in [1] <sup>1</sup>. In Fig. 3 we plot the corresponding results for the same three distributions as in Fig. 2. As expected, the distribution of  $E_T^{(1)}$  now behaves physically down to  $E_c + \delta$ , as do those of  $E_T^{(2)}$  and  $\overline{E}_T$ . However, whereas the first distribution ends there, the other two continue below  $E_c$ . Both of them are, however, singular at  $E_T^{(2)} = \overline{E}_T = E_c$ , diverging at this point from left to  $+\infty$  due to the divergence of real emission contributions as  $E_T^{(2)} \to E_T^{(1)}$ . However, as in the case of the symmetric cuts, the integrals over the distributions in Fig. 3 are finite and the same. The behaviour of the distributions of  $E_T^{(2)}$  and  $\overline{E}_T$  below  $E_c$  is of course as unphysical as the negative values of the distributions of  $E_T^{(1)}$  and  $\overline{E}_T$  closely above  $E_c$  in the symmetric cut scenario of Fig. 2.

<sup>1</sup> Instead of (6) slightly different modification of (5) was used even earlier in [4].

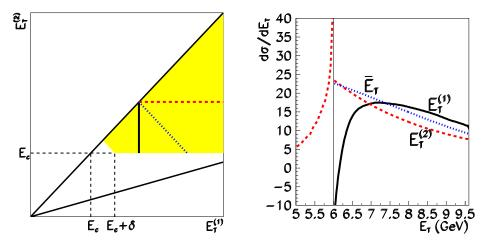


Fig. 4. The same as in Fig. 2 but for the sum cuts scenario with  $E_c = 5$  GeV and  $\delta = 2$  GeV.

Moreover, it is simple to invent an additional constraint that cuts off part of the phase space region defined in (6) in a similar way as the condition  $E_T^{(1)} \geq E_c + \Delta$  in the case of the symmetric cut. For instance the restriction

$$E_T^{(2)} \le 2E_T^{(1)} - E_c - \delta - \Delta,$$
 (7)

which cuts off part of the region (6) as shown in the middle right picture in Fig. 1 results in the integrated cross section  $\sigma_{asym}(\Delta)$  exhibiting the same kind of unphysical behaviour for  $\Delta \to 0$  as  $\sigma_{sym}(\Delta)$ .

Sum cut scenario

The cuts on  $E_T^{(1)}, E_T^{(2)}$  can also be formulated in terms of their mean value

$$\overline{E}_T \equiv \frac{E_T^{(1)} + E_T^{(2)}}{2} \ge E_c + \frac{\delta}{2}, \quad E_T^{(2)} \ge E_c.$$
 (8)

As shown in Fig. 4 in this case it is the distributions in  $E_T^{(1)}$  and  $E_T^{(2)}$  that are singular at  $E_c$ : the former turns negative and diverges when  $E_T^{(1)}$  approaches  $E_c$  from above, whereas the latter diverges to plus infinity for  $E_T^{(2)} \to E_c$  from below. As in the previous two cases the integrals over all three distributions are, however, finite and the same.

Although even for the lowest  $\overline{E}_T$  the region defined in (8) involves integration over finite neighbourhood of the point  $E_T^{(1)} = E_T^{(2)}$ , this scenario was claimed in [5] not to be infrared safe. The argument was based on the fact that similarly as in the case of the symmetric cut scenario (5) the integrated cross section  $\sigma_{sum}(\Delta)$ , corresponding to the additional constraint  $E_T^{(1)} \geq E_c + \delta/2 + \Delta$  behaves, as illustrated by the green dashed curve in Fig. 1, unphysically for  $\Delta \to 0$ . However, as emphasized above, the same objection can actually be raised against any scenario. This is clear from the geometrical meaning of the additional cuts involving the parameter  $\Delta$ : as shown in the right part of Fig.

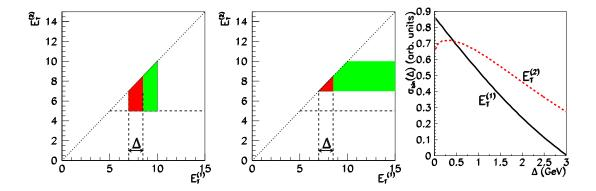


Fig. 5. The effects of the cutting the bin defined in (9-10) according to (11) on the distributions in  $E_T^{(1)}$  and  $E_T^{(2)}$ .

1, in all three scenaria it cuts off the peaks of the wedges in the plane  $E_T^{(1)}, E_T^{(2)}$ where the negative infinities of the virtual corrections dominate.

The scenario (8) is often supplemented with a constraint on the relative difference of jet transverse energies, for instance,  $(E_T^{(1)} - E_T^{(2)})/(E_T^{(1)} + E_T^{(2)}) \le 1/4$ . This cuts off part of the three jet phase space but as indicated by the black dash-dotted curve in Fig. 1, has only small effect of the behaviour of  $\sigma_{sum}(\Delta)$ .

The results presented in Figs. 1-4 demonstrate that there is no real advantage of the asymmetric or sum-like cut scenaria over the symmetric one. All of them suffer from the same kind of unphysical behaviour of two of the three distributions in  $E_T^{(1)}$ ,  $E_T^{(2)}$  or  $\overline{E}_T$  and all three can be supplemented by additional constraints that lead to the same unphysical dependence on integrated cross sections  $\sigma_{sym}(\Delta)$ ,  $\sigma_{asym}(\Delta)$ , or  $\sigma_{sum}(\Delta)$  displayed in Fig. 1.

## Distributions in bins of finite width

In practice experimental distributions in  $E_T^{(1)}, E_T^{(2)}$  and  $\overline{E}_T$  have finite bin widths. For each bin of these variables we can introduce an additional cut  $\Delta$ , which chops off part of this bin, and investigate the dependence of the bin content on this parameter in the limit  $\Delta \to 0$ , much in the same way as we did above for the integrated cross sections. Note that for  $E_T^{(1)}, E_T^{(2)} \geq E_c + \delta$ the choice of the cut scenario is irrelevant for these considerations as it does not influence the distributions there. Let us take as an example the bin

$$7 \le E_T^{(1)} \le 10 \text{ GeV}, \quad E_T^{(2)} \ge E_c$$
 (9)  
 $7 \le E_T^{(2)} \le 10 \text{ GeV}, \quad E_T^{(1)} \ge E_T^{(2)}$  (10)

$$7 \le E_T^{(2)} \le 10 \text{ GeV}, \quad E_T^{(1)} \ge E_T^{(2)}$$
 (10)

represented in left two pictures of Figs. 5,6 by the vertical and horizontal colored bands. We first introduce the parameter  $\Delta$  similarly as for the symmetric cut (6) by imposing additional constraint:

$$7 + \Delta \le E_T^{(1)} \le 10 \text{ GeV}$$
 (11)

which means graphically cutting off the red areas in Fig. 5. The resulting  $\Delta$ -dependence of the contributions  $d\sigma/dE_T^{(1)}$  and  $d\sigma/dE_T^{(2)}$  to the corresponding bin content  $\sigma_{bin}(\Delta)$ , displayed in the right part of Fig. 5, shows that the distribution of  $E_T^{(2)}$  behaves unphysically for small  $\Delta$ , whereas that of  $E_T^{(1)}$  increases monotonously as  $\Delta \to 0$ .

However, we can cut off part of the bin (9-10) in an alternative way represented by the red areas in Fig. 6

$$7 \le E_T^{(2)} \le 10 - \Delta \text{ GeV},$$
 (12)

which is certainly as legitimate as the cut (11). The corresponding results, shown in the right part of Fig. 6, lead, however, to opposite conclusion! Now it is the  $d\sigma/dE_T^{(2)}(\Delta)$  distribution that is a monotonously decreasing function of  $\Delta$ , whereas  $d\sigma/dE_T^{(1)}(\Delta)$  exhibits much the same unphysical dependence on  $\Delta$  as did  $d\sigma/dE_T^{(2)}(\Delta)$  for the cut defined in (11).

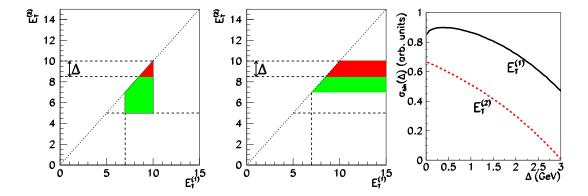


Fig. 6. The same as in Fig. 5 but for the cut defined in (12).

In summary, for dijet sample there is thus no way how to introduce the cuts on the jet transverse energies that would avoid entirely the problem noted in [1]. Whatever variables, quantity and binning we choose, there is always a simple way how to cut the chosen kinematical region in a way that leads to the same sort of unphysical behaviour of cross sections shown in Fig. 1 and the asymmetric cut scenario is therefore not superior to the symmetric one. On the other hand the above exercise also suggest a simple cure: one just needs to choose the appropriate variable or take sufficiently wide bins in jet transverse energies.

We are grateful to G. Grindhammer and V. Shekelyan for raising the questions that initiated this investigation. This work was supported in part by the project LN00A006 of the Ministry of Education of the Czech Republic and by the Institutional research project AV0Z1-010-920.

# References

- [1] S. Frixione, G. Ridolfi, Nucl. Phys. B 507 (1997) 315.
- [2] C. Adloff et al. (H1 Collaboration), in preparation
- [3] S. Catani, M. H. Seymour, Nucl. Phys. B 485 (1997) 291.
- [4] M. Klasen, G. Kramer, Phys. Lett. B 366 (1996) 385.
- [5] B.Pötter, Comp. Phys. Commun. 133 (2000) 105.